**Final Report on**

# Combustion of Oil and Water-in-Oil Emulsion Layers Supported on Water

***Grant no. 60NANBD0036***

for the period 4/1/98 to 5/31/00

*Submitted to*:

Doug Walton
National Institute of Standards and Technology
US Department of Commerce
*and*
Sharon Buffington and Joseph Mullin
Mineral Management Service
US Department of Interior

by

Anil K. Kulkarni
Department of Mechanical Engineering
204 Reber Building
The Pennsylvania State University
University Park, PA 16802
(814 865 7073) email : akk@psu.edu

August 2000

**For Contractual Matters Please Contact:**
Paul Antolosky
Office of Sponsored Programs
110 Technology Center Building
University Park, PA 16802
(814) 863-0681 e-mail: PANTOL1@rtto.psu.edu

# Table of Contents

## Executive Summary

This is the final report on grant no. 60NANBD0036 for the period 4/1/98 to 5/31/00.

The goal of the research program was to broaden the current understanding of combustion of oil and water-in-oil emulsion layers on water, and then apply that knowledge to further the acceptance and use of in-situ burning cleanup technique. The idea is to define, and possibly widen, the window of opportunity for the application of in-situ burning as a primary response countermeasure for oil spill cleanup. The specific tasks were (i) to conduct burn tests on emulsions of three oils, diesel, Milne Point crude (MPU) and Alaska North Slope crude (ANS), for a range of external heat fluxes, water content in the emulsions, and weathering; and (ii) to develop a mathematical model for the process.

In the burn tests, crude emulsions ranged from 0 to 80 % water content, the external radiant heat flux ranged from 0 to 20.8 $kW/m^2$, and the weathering ranged from 0 to 26%. Measurements included threshold (minimum) heat flux needed to achieve sustained burning of the emulsion, burn period, average burning rate, residue volume, flame height of pool fire and transient in-depth temperature profile. A comprehensive model was developed based on fundamental heat transfer equations, constitutive relations, and known property data. The model was solved numerically and model results were compared with some of the experimental data.

It was shown that the emulsion burning is very sensitive to the external heat flux. Below a certain threshold heat flux value ignition is impossible, but slightly above that value, it burns well, with reasonable removal efficiency. This supports our hypothesis that a normally incombustible emulsion of water-in-oil can be made to burn if a pool fire of sufficient size is present adjacent to it (which provides a heat flux greater than the threshold level). Additional data on other crude oils will be very useful.

Following is a list of publications and reports developed as a result of the grant.

Walavalkar, A. and Kulkarni, A. K., 1998, In-situ Burning of Water-in-Oil Emulsions: Model Results and Comparison with Data, presented at the NIST Annual Conference on Fire Research.

Walavalkar, A. and Kulkarni, A. K., 1998, Comparison of Model Predictions with Experimental Data on Combustion of Water-in-oil Emulsions Supported on Water, presented at the *Twenty First Arctic and Marine Oil-spill Program Technical Seminar*, June 1998, Vancouver, Canada.

Benson, Jennifer, 1998, Water-in-Oil Emulsion Property and Combustibility Analysis, final report on NSF-Research Experience for Undergraduates program, Department of Mechanical Engineering, The Pennsylvania State University.

Oakes, Brad, 1999, ME 496 course report on Diesel-water Emulsion Combustion Supported on Top of Water, submitted to Department of Mechanical Engineering, The Pennsylvania State University.

Walavalkar, A. Y., PhD thesis on Study of Water-in-oil Emulsions Floating on Top of Water, expected completion May 2001, Department of Mechanical Engineering, The Pennsylvania State University.

Walavalkar, A. Y., and Kulkarni A. K., 2000, Combustion of Water-in-oil Emulsion Layers Supported on Water, submitted for review to *Combustion and Flame*.

Walavalkar, A. Y., and Kulkarni A. K., 2000, Combustion of Water-in-oil Emulsion Layers Supported on Water, presented at the *'National Heat Transfer Conference'*, August 2000.

Walavalkar, A. Y., and Kulkarni A. K., 2000, "Combustion of Floating, Water-in-oil Emulsion Layers Subjected to External Heat Flux", proceedings of the *Twenty Second Arctic and Marine Oil-spill Program Technical Seminar*, Vancouver, Canada, 2000, pp 847-856.

## Introduction

In-situ oil spill combustion can be a highly effective clean up measure for contained spills occurring on open water bodies, such as an oil spill on the ocean contained by booms or a spill surrounded by ice. When feasible, it is an inexpensive technique that can have a very high efficiency of removal (possibly greater than 99%), and the spill removal rate is very rapid compared to those of mechanical means. Also, ecological damage from the spill combustion has been found to be less severe compared to that from conventional methods. (Fingas and Laroche, 1990; Evans and Tennyson, 1991). However, the window of opportunity for applying the technique is often limited for several reasons. For example, the wave and wind conditions may be too severe for ignition, the spill may be too close to populated areas, or the oil may mix with water to form emulsions that are difficult to ignite or burn. Extensive studies by Buist and McCourt, 1998, Bech *et al*., 1992, Guenette *et al.*, 1994, and Guenette *et al.*, 1995 have shown that stable emulsions with greater than a certain amount of water do not burn.

It has been known in the field of fire research that several materials, such as most woods and certain plastics, do not sustain fire on a small scale unless assisted by external heat flux. A large fire returns a significant amount of heat back to the burning area and also to the yet-to-be–ignited area, allowing fire to sustain and spread. Prior work shows that, when a material (normally incombustible in the absence of external heat flux) is subjected to a minimum (also known as threshold or critical) heat flux, it can be ignited, and a sustained fire and flame spread can be achieved (Brehob and Kulkarni, 1998). In the present work, this principle is applied to the oil spill and emulsion combustion problem. If successful, the window of opportunity for in-situ combustion of emulsions can be widened.

The important question is, how can an emulsion pool be subjected to external heat flux when it is floating on an open water body? Among other possibilities, it is proposed here that the external heat flux may come from an adjacent pool fire as shown in Figure 1. A small pool fire will not produce sufficient heat flux, but if the pool size is sufficiently large, it will provide the needed minimum heat flux for the surrounding emulsion to ignite and burn. This will make the pool size and fire size grow, provide an even larger heat flux to the yet-unburned emulsion around the pool, cause the mixture to

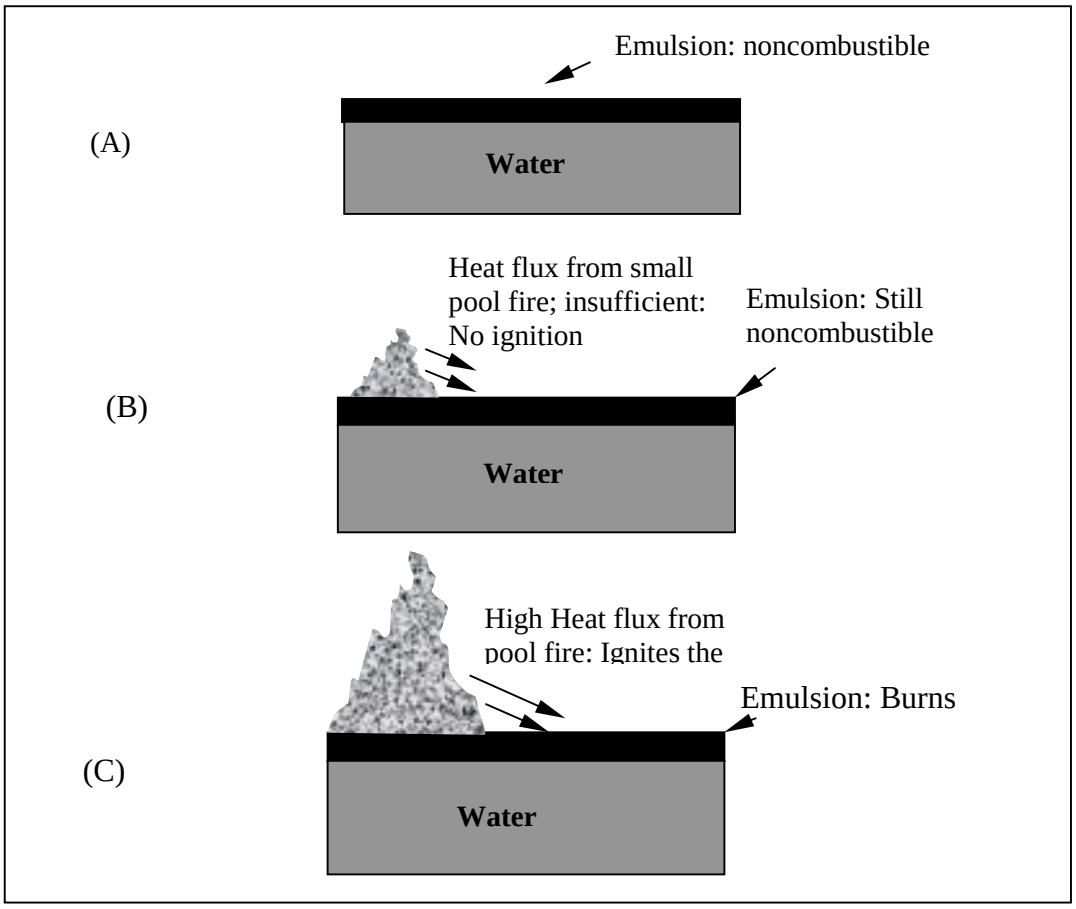


Figure 1 A noncombustible oil-water emulsion (A) can not be ignited with heat flux less than the threshold heat flux value (B), but it may be ignited with high heat flux from an adjacent pool fire of sufficiently large size (C).

ignite and continue to burn, and the process will continue. Thus, the emulsion layer, which was considered noncombustible, can now be burnt with this technique.

The initial pool fire of desired size might be achieved by one of several different means, such as, intentionally starting a fresh oil fire, using a special large size igniter, using artificial external heat flux, etc. Correlation of the radiant heat flux as a function to the surrounding area of the fire size depends on the type of fuel and other factors, such as how much soot the flames produce and the height of flames. Heat feedback from a known size of pool fire to its base has been modeled (see, for example, Tien, 1985), and measured for large fires (see, for example, Yamaguchi and Wakasa, 1986).

The scope of the current work is limited to studying the ignition and combustion behavior of fresh and weathered crude oil emulsions under external heat flux. The size and other characteristics of adjacent fires that may supply the heat flux will be a subject of later investigation (which has also been discussed to some extent in the literature). The specific objective of the current work is to conduct burn tests on emulsion pools of diesel, Milne Point (MPU) crude, and Alaska North Slope (ANS) crude, for a range of external heat fluxes, water content in the emulsions, and weathering conditions. These three fuels were selected because they have been studied extensively by Buist and McCourt, 1998 in similar types of experiments but with no external heat flux. Measurements include the threshold (minimum) heat flux needed to achieve sustained burning of the emulsion, burn period, average burning rate, and residue volume.

# Experiments

## Setup

The set up was designed and instrumented to take data from a pool fire of water-in-oil emulsion floating on top of water. The schematic of the pool fire set up is shown in figure 2. A 28 cm x 28 cm size pool was placed in the center of a 150 cm x 120 cm x 25 cm deep, water pool. The central pool is contained inside the outer pool by metal bars. The emulsion is poured in the center pool to a desired thickness on top of the water to produce a 15 mm fuel layer. The outer water pool is needed for protection from accidental spillover and flame spread from the fuel. For visual accessibility to the fire, the outer tank is made of clear acrylic. Emulsions of different oils and various compositions were made using a separate custom built apparatus based on the technique of end-over-end rotation (Hokstad *et al.*, 1995) of cylinders containing water and oil mixtures of desired proportion for up to 48 hours.

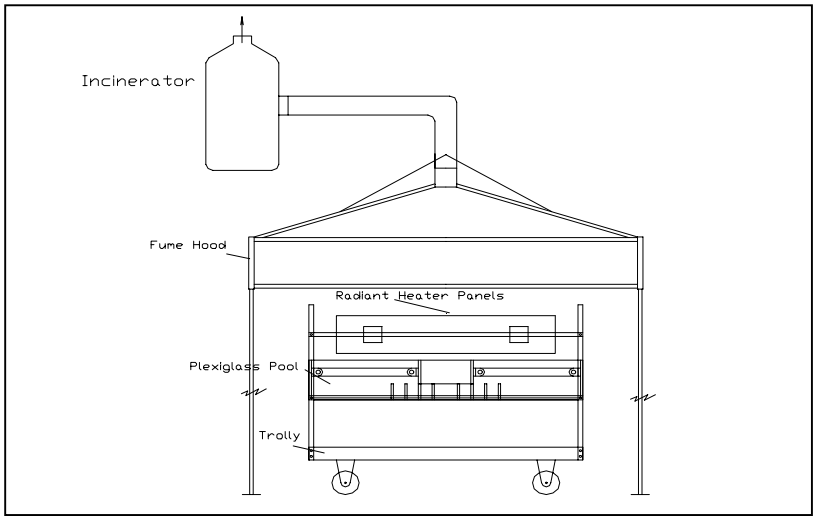


Figure 2. Schematic of Pool Fire Set-up

Two electrically operated heating panels were used to supply external radiation. The panels have rows of heating elements embedded in a ceramic material and have a Corning Vycor face plate. They are electrically heated by 440 V, three phase, 60 amp

power and controlled by a silicon control rectifier (SCR), which allows the panels to reach a maximum temperature of 815 °C that produce a maximum radiative heat flux of about 60 kW/m$^2$ at the panes. The panels were mounted facing toward the pool at an angle of 30° to vertical to irradiate the oil/emulsion pool with a uniform heat flux. Based on the geometry and view factor estimated, the fuel pool was subjected to a radiative heat flux of up to 22 kW/m$^2$. Depending on the requirements, as the experiments progressed, this maximum radiative heat flux level was changed by raising or lowering the panels. Calibration of the heater panels was made using a 12.7 mm diameter, water-cooled circular foil heat flux gage. For the calibration, twelve locations were chosen to cover the emulsion pool surface and measurements were taken at steady state. The average of the twelve readings for a particular setting of the controller was considered as the heat flux on the emulsion pool surface at that controller setting. The maximum and minimum heat flux measurements for any particular setting were within ± 5 % of the average heat flux value at that setting.

The entire pool assembly was mounted on a movable base and covered with a flame hood. The hood outlet was connected to a down-fired combustor (DFC) through an electric blower. The exhaust of the pool fire was burned in the DFC. Ignition of the pool was achieved by use of either 11 in long matchsticks supported at the front end of a wooden rod or a small natural gas pilot flame close to the emulsion surface.

Type K thermocouples were used to monitor the in-depth temperature distribution and temperature at the oil-water interface. A rake of five thermocouples with a spacing of 5 mm between consecutive thermocouples was mounted inside the inner pool. A 16-channel data acquisition board was used to collect the temperature data during the burn and the data was stored on a PC.

A video camera was used to record the test runs. These measurements were needed to determine the flame height, the conditions at which ignition took place (or did not take place), provide input to numerical models, and in general, understand the interdependence of the variables (for example, the relation between heat flux and burn rate). The data will also be used to generate dependence of average flame height on various other factors, such as water content of the emulsion, weathering, and incident radiant heat flux. The flame height data can in turn be related to the heat flux distribution on the pool surface surrounding the fire.

**Test Procedure**

In a typical test run, a predetermined amount of emulsion was poured evenly over the center section of the water in the pool fire set-up shown in figure 2. The radiation heater panels were then turned on to a known heat flux setting with the emulsion pool covered so that the pool did not receive any heat flux till the panels reached steady state. It was noted during the heater panel calibration that the panels reached steady state in about 5 minutes after being turned on. The pool was uncovered and exposed to the panel radiation after the panels were at steady state. After the surface temperature reached a certain preset value, an attempt was made to ignite the sample. Upon failure to cause ignition, the heat flux level of the panels was increased by a small amount. The process was repeated until sustained combustion was achieved, and the minimum or critical heat flux needed to ignite the sample was noted. When the fire extinguished, the volume of the residue was measured. Based on the initial volume of emulsion poured and the total time of burn, the average oil burning rate value was calculated.

Burn tests were conducted with emulsion pools of diesel, Milne Point (MPU) crude, and Alaska North Slope (ANS) crude. A small amount of either SAE30 motor oil (10% by volume) or MPU crude (5% by volume) had to be added to the mixture to promote emulsification for some of the oils. Stability was determined by how long the emulsion holds without breaking; the unstable emulsions separated into water and oil quickly. The emulsion was considered to be stable if there was no visible separation of the water and oil phases of the emulsion by the time the test run was over. It should be noted that the emulsions were probably not “truly”stable, in the sense that they would not last several days or months without separating. However, in a practical situation of an oil spill on ocean, one may expect partial emulsification to take place before applying the spill combustion technique. In a typical test run, the emulsion was used in about 24 hours after it was made.

**Preliminary Results**

Figure 3 shows fire from burning fresh oils (not weathered or mixed with water). Diesel takes the longest to ignite and it produces the most soot among the three oils tested. ANS crude ignites almost instantly and it has the tallest flames. The Milne Point (MPU) crude has the shortest flames and produces the least amount of soot.

(A) (B) (C)

Figure 3. Fires produced by burning fresh ANS (A), Diesel (B), and MPU (C).

**Test Results for Diesel**

Diesel does not form stable emulsions even after vigorous mixing for 48 hours and therefore, a small amount of either SAE30 motor oil (10% by volume) was added to the mixture to promote stable emulsification. This method resulted in sufficiently stable emulsions that would not separate till the test.

Test matrix for the diesel tests is presented in Table 1, which shows the composition of the fuel mixture, external radiant flux, and comments regarding the combustibility of the sample for each test run. Table 2 shows the reduced data for the diesel tests, indicating ignition delay, burn time, residue volume, average flame height, and burn rate.

| Test No | Emulsion Composition, % by volume | | | Radiant Heat Flux ($kW/m^2$) | Comments |
|---|---|---|---|---|---|
| | Diesel | Water | SAE 30 | | |
| 1 | 40 | 50 | 10 | **4.43** | **Ignition** |
| 2 | 50 | 40 | 10 | **8** | **Ignition** |
| 3 | 50 | 40 | 10 | 0 | No Ignition |
| | | | | 3.07 | No Ignition |
| | | | | **3.9** | **Ignition** |
| 4 | 40 | 50 | 10 | **3.6** | **Ignition** |
| 5 | 30 | 60 | 10 | 3.6 | No Ignition |
| | | | | **3.9** | **Ignition** |
| 6 | 60 | 30 | 10 | 3.07 | No Ignition |
| | | | | **3.3** | **Ignition** |
| 7 | 20 | 70 | 10 | 3.07 | No Ignition |
| | | | | 3.3 | No Ignition |
| | | | | **3.6** | **Ignition** |
| 8 | 10 | 80 | 10 | 3.3 | No Ignition |
| | | | | 3.6 | No Ignition |
| | | | | 3.9 | No Ignition |
| | | | | 4.2 | No Ignition |
| | | | | 4.45 | No Ignition |
| | | | | **6.02** | **Ignition** |
| 9 | 10 | 80 | 10 | 4.45 | No Ignition |
| | | | | 4.75 | No Ignition |
| | | | | 5.05 | No Ignition |
| | | | | 5.4 | No Ignition |
| | | | | **5.7** | Weak Ignition, Quick Extinction |
| | | | | **6.02** | **Ignition** |
| 10 | 20 | 70 | 10 | **3.3** | **Ignition** |
| 11 | 40 | 50 | 10 | ? | Ignition. Improper Heater Panel control |
| 12 | 80 | 10 | 10 | ? | |
| 13 | 40 | 50 | 10 | 2.4 | No Ignition |
| | | | | 3 | No Ignition |
| | | | | **3.6** | **Ignition** |
| 14 | 70 | 20 | 10 | 1.4 | No Ignition |
| | | | | 1.9 | No Ignition |
| | | | | **2.4** | **Ignition** |
| 15 | 50 | 40 | 10 | 2.4 | No Ignition |
| | | | | 3 | No Ignition |
| | | | | **3.6** | **Ignition** |
| 16 | 80 | 10 | 10 | 1.4 | No Ignition |
| | | | | 1.9 | No Ignition |
| | | | | **2.4** | **Ignition** |

Table 1. Test matrix for the diesel tests

| Water in Emulsion % | Heat Flux kW/m$^2$ | Burn Time second | Ignition Delay second | Residue ml | Oil Residue Thickness mm | Burn Rate mm/s |
|---|---|---|---|---|---|---|
| 80 | 6.02 | 106 | 20.8 | 320 | 0.41 | 0.009 |
| 70 | 3.60 | 244 | 35.0 | 700 | 1.79 | 0.005 |
| 60 | 3.90 | 405 | 20.0 | 600 | 2.31 | 0.005 |
| 50 | 3.60 | 475 | 0.0 | 580 | 2.97 | 0.006 |
| 40 | 3.60 | 556 | 51.0 | 790 | 5.05 | 0.004 |
| 40 | 3.90 | 612 | 0.0 | 405 | 2.59 | 0.008 |
| 30 | 3.30 | 765 | 15.0 | 365 | 2.81 | 0.008 |
| 20 | 2.40 | 746 | 36.0 | 390 | 3.50 | 0.009 |
| 10 | 2.40 | 761 | 48.0 | 480 | 4.92 | 0.009 |

Table 2. Reduced data for diesel tests

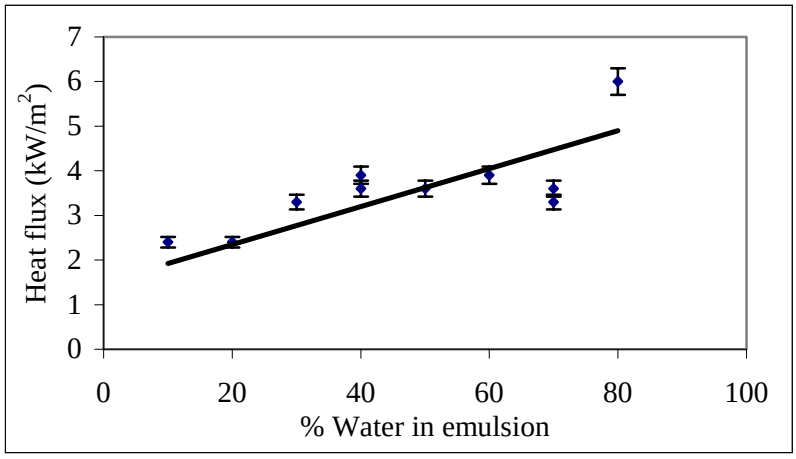


Figure 4. Minimum Heat Flux Required to Cause Sustained Fire as a Function of Water Content of Diesel-Water Emulsion.

Figure 4 shows the variation of the minimum heat flux value required to cause the sustained combustion of the emulsion as a function of the water content of the emulsion for diesel. The critical heat flux values were estimated to have an uncertainty of about ±0.6 kW/m$^2$ in addition to a non-uniformity of ± 5% around the mean values reported. The scatter in data best indicates the overall uncertainty in other experimental values. It is estimated to be about 4% for the burn time measurements, 11% for the residue thickness measurements and 9% for the burn rate measurements. The heat flux value plotted is the average heat flux incident on the surface of the emulsion pool. Error bars indicate a variation from the average heat flux value at the surface. The minimum

heat flux necessary to cause sustained fire increased with increasing water content of the emulsion. These results show that normally incombustible emulsions can be made to burn if there is sufficient external heat flux, and thus the window of opportunity for use of in-situ burning technique can be widened.

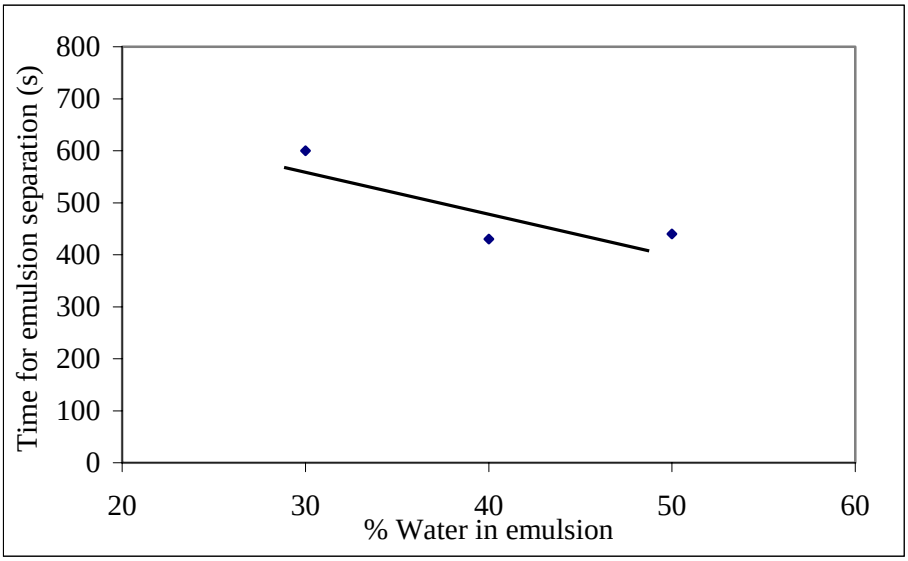


Figure 5. Time for Emulsion Separation as a Function of Water Content of the Diesel-Water Emulsion at Critical Heat Flux.

Figure 5 shows the time for emulsion separation as a function of water content of the emulsion for diesel. These results were obtained at the external heat flux value equal to the critical heat flux. Here, 90 °C was used as the emulsion separation temperature, and the time it took for the top surface of the emulsion to reach 90 °C was noted. The separation temperature was based on experimental observations made in our lab tests (Pisarchik *et al*., 1997). Guenette *et al*. (1995) have argued that is the oil vapor, not the liquid oil itself, which actually burns. Thus, the ignition delay includes the total period required to heat the emulsion, separate it into oil and water, heat the oil to evaporation temperature, evaporate the oil, mix the vapor and oxidizer from air, and then start the combustion reaction of the mixture. The largest fraction of time in the ignition delay is probably up to the separation of emulsion into oil and water. Thus, the emulsion separation period is closely related to the ignition delay. The ignition delay itself was not calculated, nor measured, because the ignition delay was hard to define precisely in the

present setup. It will be somewhat dependent upon the position of the igniter (because the process is not strictly one-dimensional) and the "flashing" phenomenon occurring before sustained ignition.

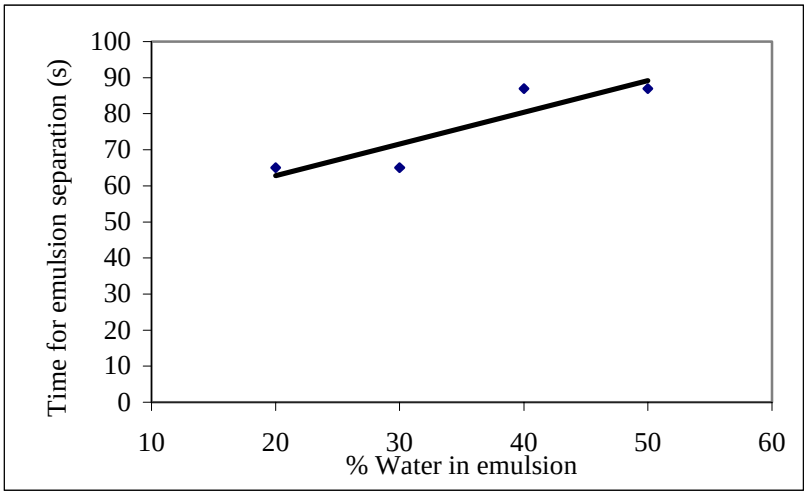


Figure 6. Time for Emulsion Separation as a Function of Water Content of the Emulsion at a Constant Heat Flux of 8 kW/m$^2$.

Figure 6 shows the time for emulsion separation as a function of water content of the emulsion at a constant incident heat flux of 8 kW/m$^2$ for diesel. At a constant external heat flux, time for emulsion separation increases with increasing water content of the emulsion. The probable reason is, as the water fraction of emulsion increases, the thermal diffusivity of the emulsion layer increases. This means that the emulsion layer is now conducting more of the heat received. Thus it takes more time for the surface temperature to reach the emulsion breaking temperature.

Figure 7 shows the average burning rate for diesel as a function of water content of the emulsion at critical heat flux. Overall, the average burning rate decreases with increasing water content of the emulsion. The average burning rate at critical heat flux is a combination of two opposing factors. With more water in the emulsion, there is less amount of diesel separated from the same amount of emulsion. Thus the diesel available for burning is provided at a slower rate from the emulsion layer. Hence the diesel-burning rate is lower. However, the critical heat flux itself increases with increasing water fraction (see figure 4), enhancing the rate of emulsion separation into diesel and

water. The net effect, as shown in figure 7, is to somewhat slow down the burning rate with increasing water fraction of the emulsion at the critical heat flux.

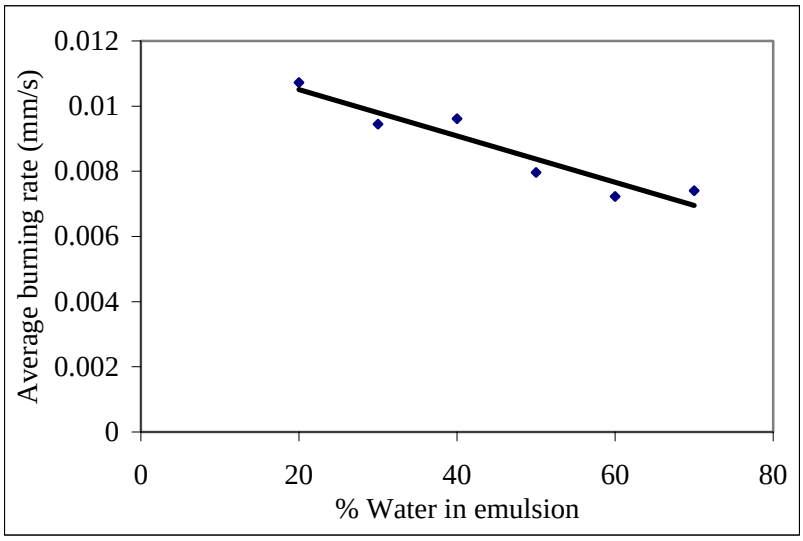


Figure 7. Average Diesel Burning Rate as a Function of Water Content of the Emulsion at Critical Heat Flux.

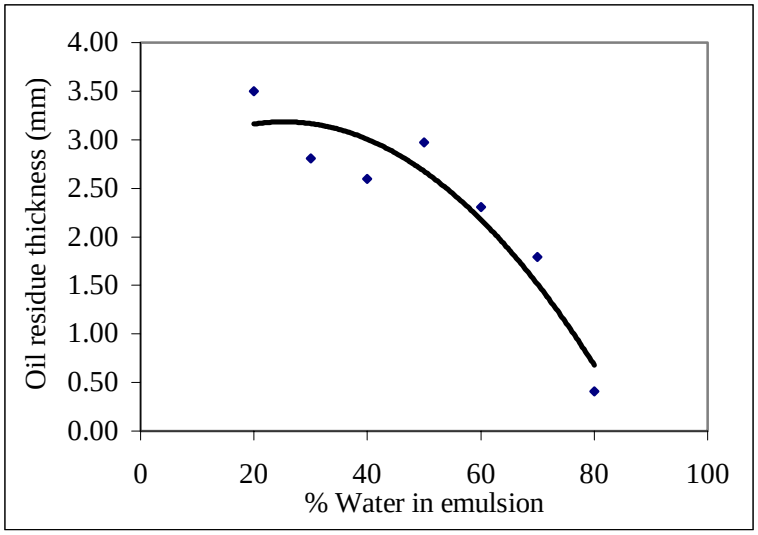


Figure 8. Diesel Residue Thickness as a Function of Water Content of the Emulsion at Critical Heat Flux.

Figure 8 shows the experimentally measured diesel residue thickness values as a function of water fraction of the emulsion. The residue thickness decreased with increasing water fraction in the emulsion. With more water in the emulsion, there was

less amount of diesel to start with. Hence the diesel residue decreased with increasing water fraction of the emulsion.

**Test Results for MPU Crude**

MPU mixed with water very quickly (less than 8 hours) to form a very stable emulsion. The emulsion was considered to be stable if there was no visible separation of the water and oil phases of the emulsion by the time the test run was over. It should be noted that we *were* able to make emulsions with fresh and weathered MPU, which is in contrast with the experience of Buist and McCourt (1998) who found it very difficult to make emulsions with MPU. We have not been able to resolve the discrepancy as yet, but we are further exploring it. Table 3 shows test conditions for MPU crude tests.

Figures 9 and 10 show variation of critical heat flux for fresh and weathered MPU emulsions having a range of water content. It was noted that the MPU emulsions needed greater heat flux to burn compared to the diesel emulsions of same water content. A greater threshold heat flux is needed to burn the fuel if it is weathered more and/or has a higher content of water. In any case, the technique of providing external heat flux to achieve burning clearly works, and seems to have a definite potential to widen the window of opportunity for in-situ burning of otherwise non-combustible mixtures.

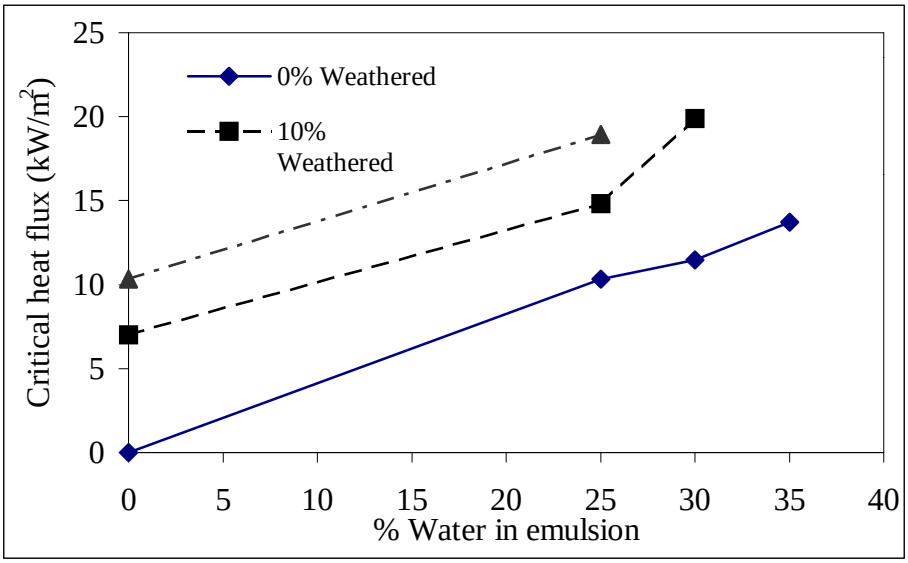


Figure 9: Variation of the critical heat flux value for the MPU-water emulsions as a function of water content of the emulsion at different weathering levels.

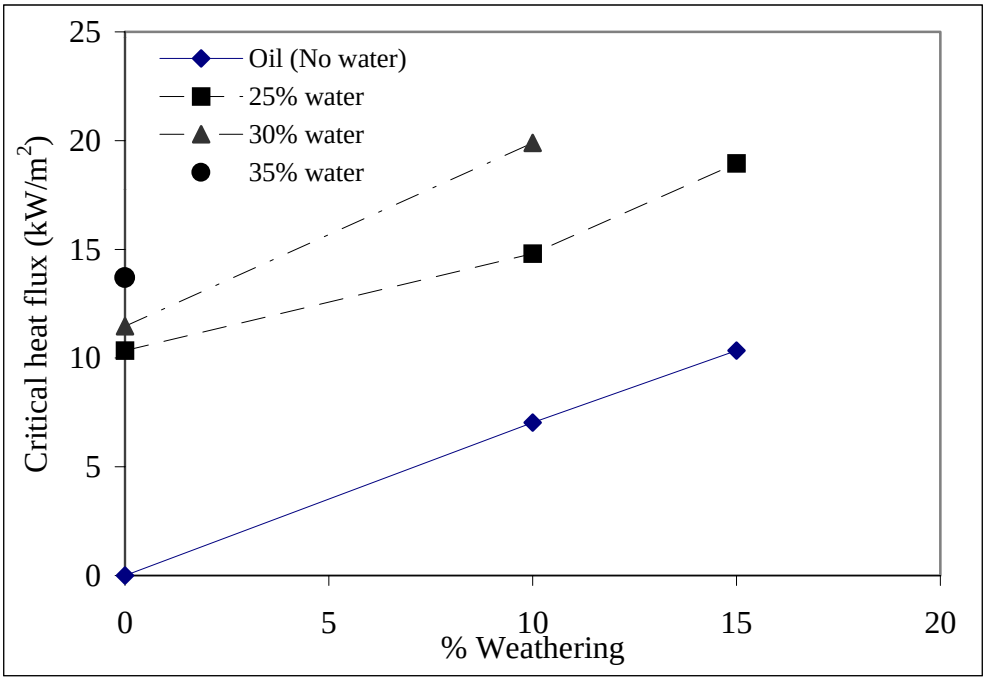


Figure 10: Variation of the critical heat flux value for the MPU-water emulsions as a function of % weathering at different levels of water content of the emulsion.

| Test No | Emulsion Composition, % by volume | | | Radiant Heat Flux ($kW/m^2$) | Comments |
|---|---|---|---|---|---|
| | %Weathering | MPU | Water | | |
| 1 | 0 | 75 | 25 | 5.0 | No Ignition |
| | | | | 7.0 | No Ignition |
| | | | | 8.1 | No Ignition |
| | | | | 9.2 | No Ignition |
| | | | | **10.3** | **Ignition** |
| 2 | 0 | 70 | 30 | 10.3 | No Ignition |
| | | | | **11.5** | **Ignition** |
| 3 | 0 | 65 | 35 | 11.5 | No Ignition |
| | | | | 12.6 | No Ignition |
| | | | | **13.7** | **Ignition** |
| 4 | 0 | 60 | 40 | 13.7 | No Ignition |
| | | | | 15.9 | No Ignition |
| | | | | 19.0 | No Ignition |
| | | | | 20.8 | No Ignition |
| 5 | 0 | 100 | 0 | **0** | **Ignition** |
| 6 | 15 | 100 | 0 | 0 | No Ignition |
| | | | | 4.9 | No Ignition |
| | | | | 9.2 | No Ignition |
| | | | | **10.3** | **Ignition** |
| 7 | 15 | 70 | 30 | 15.9 | No Ignition |
| | | | | 19.0 | No Ignition |
| | | | | 20.8 | No Ignition |
| 8 | 15 | 75 | 25 | 10.3 | No Ignition |
| | | | | 12.6 | No Ignition |
| | | | | 15.9 | No Ignition |
| | | | | 18.0 | No Ignition |
| | | | | **19.0** | **Ignition** |
| 9 | 10 | 100 | 0 | 0 | No Ignition |
| | | | | 4.9 | No Ignition |
| | | | | 6.0 | No Ignition |
| | | | | **7.0** | **Ignition** |
| 10 | 10 | 65 | 35 | 20.8 | No Ignition |
| 11 | 10 | 70 | 30 | 18.0 | No Ignition |
| | | | | **19.9** | **Ignition** |
| 12 | 10 | 75 | 25 | 13.7 | No Ignition |
| | | | | **14.8** | **Ignition** |

Table 3: Test matrix for the Milne point crude oil

**Test Results for ANS Crude**

Fresh ANS crude does not form stable emulsions even after vigorous mixing for 48 hours and therefore, a small amount of either SAE30 motor oil (10% by volume) or MPU crude (5% by volume) had to be added to the mixture to promote emulsification. Stability was determined by how long the emulsion holds without breaking; the unstable emulsions separated into water and oil quickly. It should be noted that this experience also was somewhat in contrast with that of Buist and McCourt (1998) who found it easy to make emulsions with ANS. Table 4 shows test conditions for ANS crude tests.

| Test No | Emulsion Composition, % by volume | | | Radiant Heat Flux ($kW/m^2$) | Comments |
|---|---|---|---|---|---|
| | %Weathering | ANS | Water | | |
| 1 | 0 | 75 | 25 | **0.0** | **Ignition** |
| 2 | 0 | 60 | 40 | **0.0** | **Ignition** |
| 3 | 0 | 50 | 50 | **0.0** | **Ignition** |
| 4 | 0 | 100 | 0 | **0.0** | **Ignition** |
| 5 | 26 | 100 | 0 | 0 | No Ignition |
| | | | | 2.1 | No Ignition |
| | | | | **3.0** | **Ignition** |
| 6 | 26 | 75 | 25 | 3.0 | No Ignition |
| | | | | 3.9 | No Ignition |
| | | | | **4.9** | **Ignition** |
| 7 | 26 | 60 | 40 | 6.0 | No Ignition |
| | | | | **7.0** | **Ignition** |
| 8 | 26 | 50 | 50 | 8.1 | No Ignition |
| | | | | **9.2** | **Ignition** |

Table 4: Test matrix for Alaskan North Slope crude oil.

Figure 11 shows variation of critical heat flux for fresh and weathered ANS emulsions having a range of water content. ANS-water emulsions up to 50 % water did not need any external heat flux for ignition and sustained burning. With higher water content, the fire was often very violent, splashing the mixture around. It is seen that a greater threshold heat flux is needed to burn the fuel if it is weathered more and/or has a higher content of water. More tests on weathered ANS will be useful for completeness of data. Again, the technique of providing external heat flux to achieve burning clearly works, and seems to have a definite potential to widen the window of opportunity for in-situ burning of otherwise non-combustible mixtures.

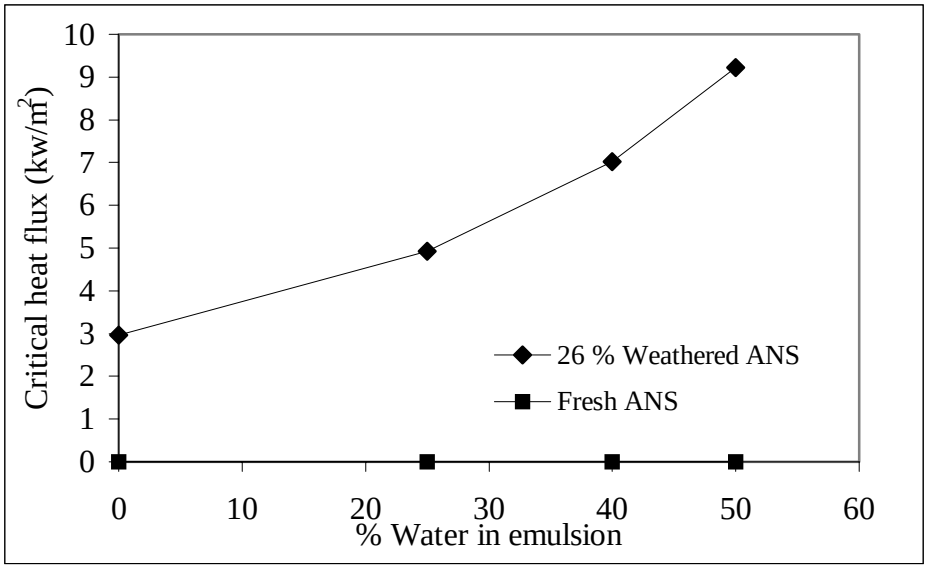


Figure 11: Variation of the critical heat flux value for the ANS-water emulsions as a function of water content of the emulsion for fresh and 26% weathered oil.

## Mathematical Model

### Background

A review of oil spill combustion studies was presented by Walavalkar and Kulkarni, 1996. The process of in-situ burning of oil or water-in-oil (w/o) emulsion supported on top of a water-base, such as the ocean, may be examined in three stages -- before, during and after the actual combustion. Events and considerations leading to spill combustion, which are very important in determining the efficacy of this technique as a cleanup countermeasure, include the evaporation or weathering of oil, emulsification with water, thickness of oil slick, ignition source, and surrounding conditions (including fire boom, waves, and wind conditions). The next stage is combustion of oil or emulsion layer -- *the primary focus of this section*. The processes in this stage are dominated by energy transfer to the layer, breakup of the emulsion layer, and subsequent burning of oil layer. The final stage is characterized by the air and aquatic pollution caused by the airborne species and the residue.

The mechanism of w/o emulsion combustion is far more complex than oil combustion. It has been postulated that it is not the emulsion that burns; rather a layer of oil separated out of emulsion and floating on top of emulsion that burns (Guenette *et al*., 1995). Thus the controlling factor in emulsion burning is the removal of water. Some experimental observations of emulsion burning reveal that (i) incident heat helps separate water and oil in emulsion (Strom-Kristiansen *et al.,* 1995) and, (ii) burn efficiencies with emulsions, even with water content as high as 50%, are in excess of 90% (Buist *et al*., 1995).

The key process in sustained combustion of the oil or w/o emulsion layer on water is the energy balance at the surface. If sufficient energy from combustion is fed back to the fuel layer, the evaporation and pyrolysis of fuel continues; if excess energy is available from combustion, flame spread and more intense burning occur; and, if insufficient energy is available, the fire extinguishes. Thompson *et al.,* 1979 proposed a simple energy balance for the oil layer burning on top of water,

$$\text{Net Energy} = 0.02\, Q_{com} - Q_{Lo} - C_{po}\,(T_{ov} - T_o),$$

where it is assumed that 2% of heat of the combustion is returned to fuel in order to compensate for the heat of evaporation and sensible heat.

Once the oil or emulsion layer is ignited, the sustained burning rate can be determined by examining the energy transfer processes at the surface at steady state. A detailed analysis of combustion of oil-emulsion layer was presented by Guenette *et al.*, 1994 which was based on the work of Brzustowski and Twardus, 1982. The burn rate for oil emulsions was given by:

$$r = \frac{q_r'' - U_o \Delta T}{\rho_O \Delta h_{v,o} + \rho_O c_{po} (T_e - T_o) - \rho_w \Delta h_{v,w} f_w / (1 - f_w)}$$

This is a steady state, zone model that allows computation of burning rate based on averaged quantities.

Putorti and Evans, 1994 made transient analysis of surface heating of viscous oils under external radiation flux for three heat loss conditions at the surface. The model was limited to a pure oil layer floating on water receiving incident radiant heat flux. Ignition delay was computed under various heat flux conditions. It was concluded, after comparing the results to experiments, that the heat transfer at the surface is dominated by convective loss at the surface, and its proper accounting allowed a better prediction of ignition time.

Wu *et al.,* 1997 analyzed combustion of fuel on water base by dividing the process into three parts, viz. ignition, flame spread and extinction. They also extended the work of Arai *et al.,* 1990 and Garo *et al.,* 1994 to obtain an expression for average regression rate using one-dimensional two-layer conduction model.

Focus of the past research in this field was primarily of experimental nature. The few attempts of modeling the process were limited in scope, such as zone models, or restricted to pure oil. Prior models did not predict the burning of *emulsions,* as they did not account for emulsion breaking mechanism. This section presents a comprehensive mathematical model for the combustion of emulsion supported by a water base. The predictions of the model are compared with the experimental observations.

**Physical Model**

In order to make the overall combustion process of an oil emulsion layer floating on top of a body of water mathematically tractable, a one-dimensional process is assumed. For the modeling purpose, it is divided into three regimes as follows,

1. *Initial Regime* ($t = 0$ to $t_1$, shown schematically in Figure 12): The model starts with the application of external heat flux to an emulsion layer floating on top of ocean surface. Entire slick is at a uniform temperature equal to the surrounding temperature. A constant radiation heat flux source is incident on the emulsion surface. The emulsion layer is heated and eventually the top surface reaches the emulsion-breaking temperature. This marks the end of initial regime.

2. *Intermediate Regime*: ($t = t_1$ to $t_2$, shown schematically in Figure 13): Continued input of heat breaks the emulsion into water and oil, which causes the first appearance of oil on top of the emulsion. Thus, there are three layers in this regime, oil, emulsion and water. The oil layer grows and the emulsion layer thins out. Now the oil layer receives incident heat flux. The oil, not being optically thick, absorbs only a part of the incident heat flux at the surface and some of the radiation energy is absorbed in-depth. The remaining heat flux that reaches the oil-emulsion interface is absorbed at the interface. The temperature of the oil layer increases while the oil-emulsion interface temperature remains constant at the emulsion breaking temperature. When the oil surface temperature reaches oil vaporization temperature, the intermediate regime ends.

3. *Final Regime*: ($t = t_2$ to $t_3$, shown schematically in Figure 14): The vaporized oil burns because of the presence of the fire, energy is released by oil combustion, and a part of it is fed back to the oil. The surface temperature of the oil now stays at the oil vaporization temperature. The vaporization causes the oil layer to deplete while the breaking up of emulsion layer causes the oil layer to grow. The process continues until the emulsion layer completely depletes, oil layer continues to burn, and finally

extinction occurs because the loss of heat (to the water and surroundings) becomes so large that enough energy is not available to cause pyrolysis of oil.

**Governing Equations**

Assumptions: The energy transfer is from the external source or igniter into the condensed phase, and in the interior, it is by one-dimensional conduction. Representative properties for emulsion are assumed to be weighted averages of the corresponding oil and water properties, and constant throughout the time of operation.

When the oil begins to vaporize and burn, the incident heat flux increases rapidly to the prescribed maximum value, $q_{max}$ (which normally depends on the type of crude oil, fire size, wind velocity, and other combustion conditions), and after that, the heat flux remains constant. Here, $q_{max}$ is assumed to be 8 kW/m$^2$, for primarily two reasons. It has been known that a significant amount flame radiation can be reflected off the oil surface depending on the incident angle, up to 60% for heptane pools at low angles. (Hamins *et al.*, 1994) The incident radiative heat flux itself varies considerably from the center to the periphery of a pool fire, for example, for a methanol fire, it is about 15 kW/m$^2$ at center to about 2 kW/m$^2$ at the periphery, and for a heptane fire, it is about 20 kW/m$^2$ at center to about 15 kW/m$^2$ at the periphery. (Hamins *et al.*, 1994) This uncertainty lead to our estimate of 8 kW/m$^2$ as absorbed (not incident) heat flux for our experiments. Also, it yielded a reasonable burn time for one of the test conditions. Therefore, $q_{max}$ was assumed to be 8 kW/m$^2$.

The separation of emulsion into water and oil is assumed to occur due to sharp decrease in surface tension of water as the temperature of water approaches the boiling point. For example, surface tension of water against air decreases from 73 dynes/cm at 20 °C to 63 dynes/cm at 80 °C nonlinearly (with rate of reduction increasing with temperature), and then continues to fall off significantly as temperature approaches the boiling point. Accurate data for temperature dependence of water surface tension against oil used in current experiments is, however, not available. Therefore, based on experimental observations made in our lab tests (Pisarchik *et al.*, 1997), emulsion is assumed to separate into water and oil at 90 °C. It is assumed that the oil separated from emulsion floats at the top and water sinks to the bottom.

Emulsion is assumed to be optically thick but oil is allowed in-depth absorption. This is because the emulsion is highly heterogeneous for the radiation wavelength and thus it is expected to be essentially opaque. The optical depth of oil is assumed to be 1.78 mm (Putorti and Evans, 1994 have reported this value for SAE 30 oil). Wind and ocean turbulence effects are neglected. Effects of aging and weathering of oil are not considered here but these effects are planned to be included in future studies.

The high viscosity of oil and very high viscosity of the emulsion (typically one or more order(s) of magnitude greater than that of the oil) allows an assumption of quiescent layers. The water below the emulsion is heated stably, and represents only a small amount of heat loss compared to the incident heat flux, therefore, the seawater base is modeled as a semi-infinite quiescent medium.

Initial Regime:

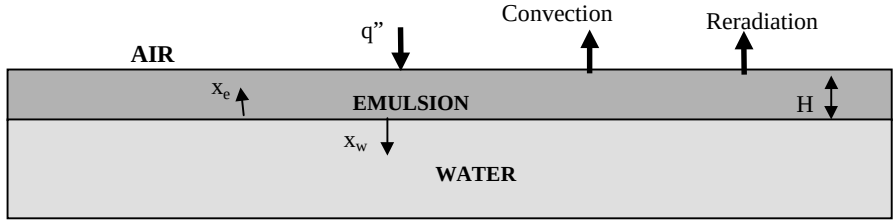


Figure 12. Initial Regime

A schematic representation of the initial regime is shown in Figure 12.

Governing Equations:

$$\frac{\partial T_{e1}}{\partial t} = \alpha_e \frac{\partial^2 T_{e1}}{\partial x_e^2} \tag{1}$$

$$\frac{\partial T_{w1}}{\partial t} = \alpha_w \frac{\partial^2 T_{w1}}{\partial x_w^2} \tag{2}$$

Initial Conditions:

$$@\ t = 0,\ T_{e1} = T_i \tag{3}$$

$$T_{w1} = T_i \tag{4}$$

Boundary Conditions:

$$@\ x_e = H,\ k_e \frac{\partial T_{e1}}{\partial x_e} = -\dot{q}'' + h_e(T_{e1} - T_i) + \sigma\varepsilon_e(T_{e1}^4 - T_i^4) \tag{5}$$

@ $x_e = 0$, $x_w = 0$,

$$k_e \frac{\partial T_{e1}}{\partial x_e} = -k_w \frac{\partial T_{w1}}{\partial x_w} \tag{6}$$

@ $x_w = \infty$, $T_{w1} = T_i$ (7)

Initial regime ends when $T_{e1} = T_{eb}$ @ $x_e = H$.

At the end of initial regime, $t = t_1$, $H = H_i$.

Intermediate Regime:

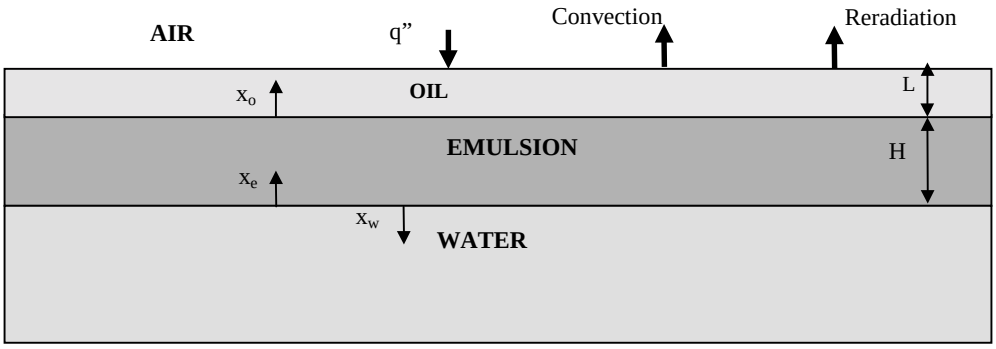


Figure 13. Intermediate Regime

A schematic representation of the intermediate regime is shown in Figure 13.

Governing Equations:

$$\frac{\partial T_{o2}}{\partial t} = \alpha_o \frac{\partial^2 T_{o2}}{\partial x_o^2} + \frac{C_0 \dot{q}'' \beta e^{-\beta(L-x_o)}}{\rho_o c_{po}} \tag{8}$$

$$\frac{\partial T_{e2}}{\partial t} = \alpha_e \frac{\partial^2 T_{e2}}{\partial x_e^2} \tag{9}$$

$$\frac{\partial T_{w2}}{\partial t} = \alpha_w \frac{\partial^2 T_{w2}}{\partial x_w^2} \tag{10}$$

Initial Conditions:

@ $t = t_1$, $T_{o2} = T_{eb}$ (11)

$T_{e2} = T_{e1}$ (12)

$T_{w2} = T_{w1}$ (13)

$L = 0$ (14)

$H = H$ (15)

Boundary Conditions and Auxiliary Conditions at the Boundaries:

@ $x_o = 0$, $T_{o2} = T_{eb}$ (16)

@ $x_o = L$,

$$k_o \frac{\partial T_{o2}}{\partial x_o} = -(1 - C_o)\dot{q}'' + h_o(T_{o2} - T_i) + \sigma\varepsilon_o(T_{o2}^4 - T_i^4) \quad (17)$$

@ $x_e = 0$, $x_w = 0$,

$$k_e \frac{\partial T_{e2}}{\partial x_e} = -k_w \frac{\partial T_{w2}}{\partial x_w} \quad (18)$$

@ $x_e = H$, $T_{e2} = T_{eb}$ (19)

@ $x_w = \infty$, $T_{w2} = T_i$ (20)

@ $x_o = 0$, $x_e = H$,

$$-k_o \frac{\partial T_{o2}}{\partial x_o} + k_e \frac{\partial T_{e2}}{\partial x_e} = aC_0\dot{q}''e^{-\beta L} \quad (21)$$

The intermediate regime ends when $T_{o2} = T_{ov}$ @ $x_o = L$.

At end if intermediate regime, $t = t_2$, $H = H_2$, $L = L_2$.

Final Regime:

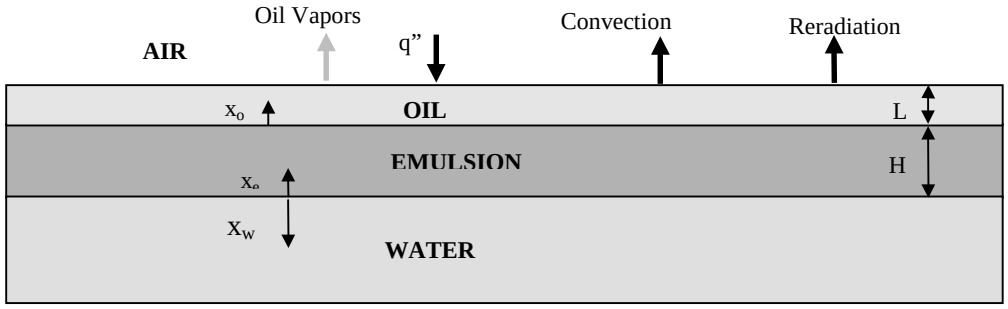


Figure 14. Final Regime

A schematic representation of the final regime is shown in Figure 14.

Governing Equations:

$$\frac{\partial T_{o3}}{\partial t} = \alpha_o \frac{\partial^2 T_{o3}}{\partial x_o^2} + \frac{C_0\dot{q}''\beta e^{-\beta(L-x_o)}}{\rho_o c_{po}} \quad (22)$$

$$\frac{\partial T_{e3}}{\partial t} = \alpha_e \frac{\partial^2 T_{e3}}{\partial x_e^2} \tag{23}$$

$$\frac{\partial T_{w3}}{\partial t} = \alpha_w \frac{\partial^2 T_{w3}}{\partial x_w^2} \tag{24}$$

Initial Conditions:

$$@\ t = t_2,\ T_{o3} = T_{ov} \tag{25}$$

$$T_{e3} = T_{e2} \tag{26}$$

$$T_{w3} = T_{w2} \tag{27}$$

$$L = L_2 \tag{28}$$

$$H = H_2 \tag{29}$$

Boundary Conditions and Auxiliary Conditions at the Boundaries:

$$@\ x_o = 0,\ T_{o3} = T_{eb} \tag{30}$$

$$@\ x_o = L,\ T_{o3} = T_{ov} \tag{31}$$

$$@\ x_e = H,\ T_{e3} = T_{eb} \tag{32}$$

$@\ x_e = 0,\ x_w = 0,$

$$k_e \frac{\partial T_{e3}}{\partial x_e} = -k_w \frac{\partial T_{w3}}{\partial x_w} \tag{33}$$

$$@\ x_w = \infty,\ T_{w3} = T_i \tag{34}$$

$@\ x_o = 0,\ x_e = H,$

$$-k_o \frac{\partial T_{o3}}{\partial x_o} + k_e \frac{\partial T_{e3}}{\partial x_e} = aC_0 \dot{q}'' e^{-\beta L} \tag{35}$$

$@\ x_o = L,$

$$k_o \frac{\partial T_{o3}}{\partial x_o} = -(1 - C_o)\dot{q}'' + h_o(T_{o3} - T_i) + \sigma\varepsilon_o(T_{o3}^4 - T_i^4) + \rho_o Q_{Lo} \frac{dL}{dt} \tag{36}$$

**Numerical Solution**

The emulsion layer was divided into 0.5-mm grid for numerical computation. The oil grid spacing was calculated in such a way that one emulsion grid formed one grid length in oil after break up. Thus the oil grid spacing was a function of the fraction of oil present in the emulsion. The grid for the water base was stretched to accommodate the semi-infinite medium using coordinate transformation. The original semi-infinite

region was transformed to a finite region in the transformed coordinate system. The transformation rule used was,

$$y_w = 1 - \frac{1}{1 + Cx_w}, \tag{37}$$

where $y_w$ is the transformed coordinate in water domain and C is stretching factor, assumed to be 0.8 here.

Explicit time accurate finite difference scheme with pseudo time stepping was used to solve the resulting set of simultaneous partial differential equations and the boundary and auxiliary conditions. A general partial differential equation selected for finite differencing can be represented as

$$\frac{\partial T}{\partial \tau} + \frac{\partial T}{\partial t} = \alpha C_{t1} \frac{\partial^2 T}{\partial x^2} + C_{t2} \frac{\partial T}{\partial x} + \frac{aC_0 \dot{q}'' \beta e^{-\beta(L-x)}}{\rho_o c_{po}} \tag{38}$$

where, $C_{t1} = C^2(1 - x)^4$ and $C_{t2} = -4\alpha_w C^2(1 - x)^3$ for water base and $C_{t1} = 1$ and $C_{t2} = 0$ for oil and emulsion layers. Also, a = 1 for oil layer to account for the in-depth radiation absorption and a = 0 for emulsion. The pseudo time ($\tau$) derivative added to the governing equation is driven to zero by attaining steady state in pseudo time, for each time step in real time (t) thus assuring a converged solution. Two-point difference in time and central difference in space is used. The code was compiled and run on SGI Irix 6.2 system. Typical run time for the code was around 20 minutes.

**Results and Comparison with Data**

For solving the model numerically, various property data values were required. Table 5 lists all the property values used as input to the numerical solution of the mathematical model. The diesel properties were obtained from Vargaftik, 1975 and Arai *et al.,* 1988.

| | Property | Value |
|---|---|---|
| Commercial No. 2 Diesel Oil | $h_o$ | 10.0 $W/m^2K$ |
| | $\varepsilon_o$ | 0.50 |
| | $k_o$ | 0.1169 W/mK |
| | $\alpha_o$ | 76.77 x $10^{-9}$ $m^2/s$ |
| | $\rho_o$ | 846 $kg/m^3$ |
| | $C_{po}$ | 1800.0 kJ/kgK |
| | $Q_{Lo}$ | 3.3 x $10^5$ J/kg |
| | $Q_{comb}$ | 4.187 x $10^7$ J/kg |
| | $T_{ov}$ | 112.0 °C |
| | $\beta$ | 560.0 $m^{-1}$ |
| Sea Water | $k_w$ | 0.67 W/mK |
| | $\alpha_w$ | 15.73 x $10^{-6}$ $m^2/s$ |
| | $\rho_w$ | 958.0 $kg/m^3$ |
| | $C_{pw}$ | 4217.0 J/kgK |
| | $Q_{Lw}$ | 2257.0 kJ/kg |
| Emulsion | $h_e$ | 10.0 $W/m^2K$ |
| | $\varepsilon_e$ | 0.95 |

Table 5. Property Value Input for the Mathematical Model

The critical heat flux values for diesel shown in figure 4 were used as input to the numerical solution of the mathematical model described earlier. Table 6 shows results of the lab scale burn experiments and the corresponding results from the model. These results were obtained at the external heat flux value equal to the critical heat flux. As described earlier, 90 °C was used as the emulsion separation temperature, and the time it took for the top surface of the emulsion to reach 90 °C was noted. This period is related to the ignition delay because the ignition occurs soon after the oil starts to vaporize. However, ignition delay itself is not calculated, nor measured, because the ignition delay is very hard to define precisely in the present setup. It will be somewhat dependent upon the position of igniter (because the process is not strictly one-dimensional) and the "flashing" phenomenon occurring before sustained ignition. Two different values of time for separation are reported in the table below, one is calculated at the critical heat flux value (which depends on the % water content) and the other at a fixed external heat flux value equal to 8 $kW/m^2$. The plots of these results are shown in figures 15-20.

The overall uncertainty in the experimental values is best indicated by the scatter in the data. It is estimated to be about 4% for the burn time measurements, 11% for the residue thickness measurements and 9% for the burn rate measurements. The critical heat flux values are estimated to have an uncertainty of about ±0.3 kW/m$^2$ in addition to a non-uniformity of ± 5% around the mean values reported.

| | Figure 19 | | Figure 20 | | Figure 18 | | Figure 15 | | Figure 16 | |
|---|---|---|---|---|---|---|---|---|---|---|
| % Water | Burn Time (s) | | Oil Residue Thickness (mm) | | Average Burn Rate (mm/s) | | Time for Emulsion Separation at Critical Heat Flux (s) | | Time for Emulsion Separation at a Constant Heat Flux of 8 kW/m$^2$ (s) | |
| | Exptl | Model | Exptl | Model | Exptl | Model | Exptl | Model | Exptl | Model |
| 20 | 746 | 695 | 3.50 | 3.48 | 0.0107 | 0.0123 | | 540 | 65 | 37 |
| 30 | 765 | 651 | 2.81 | 2.80 | 0.0095 | 0.0118 | 600 | 350 | 65 | 53 |
| 40 | 612 | 578 | 2.59 | 3.32 | 0.0096 | 0.0098 | 430 | 375 | 87 | 68 |
| 50 | 475 | 439 | 2.97 | 2.44 | 0.0080 | 0.0115 | 440 | 470 | 87 | 90 |
| 60 | 405 | 361 | 2.31 | 2.48 | 0.0072 | 0.0098 | | | | |
| 70 | 244 | 240 | 1.79 | 2.13 | 0.0074 | 0.0099 | | | | |
| 80 | 106 | 129 | 0.41 | 1.72 | 0.0206 | 0.0099 | | | | |

Table 6. Comparison of Model Predictions with Experimental Data

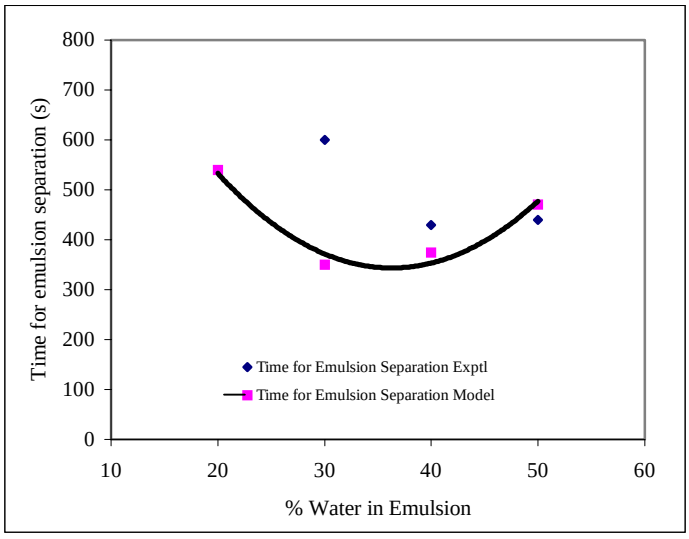


Figure 15. Comparison of model prediction of time for emulsion separation with the experimentally observed values of time for emulsion separation as a function of water content of the emulsion at critical heat flux.

Figure 15 and 16 show the time for emulsion separation as a function of water content of the emulsion at critical heat flux and at a constant incident heat flux of 8 $kW/m^2$, respectively. It can be seen that the model predictions show a trend similar to that of the experimental observations.

At a constant external heat flux, time for emulsion separation increases with increasing water content of the emulsion. This is because, as the water fraction of emulsion increases, the thermal diffusivity of the emulsion layer increases. This means that the emulsion layer is now conducting more of the heat received. Thus it takes more time for the surface temperature to reach the emulsion breaking temperature.

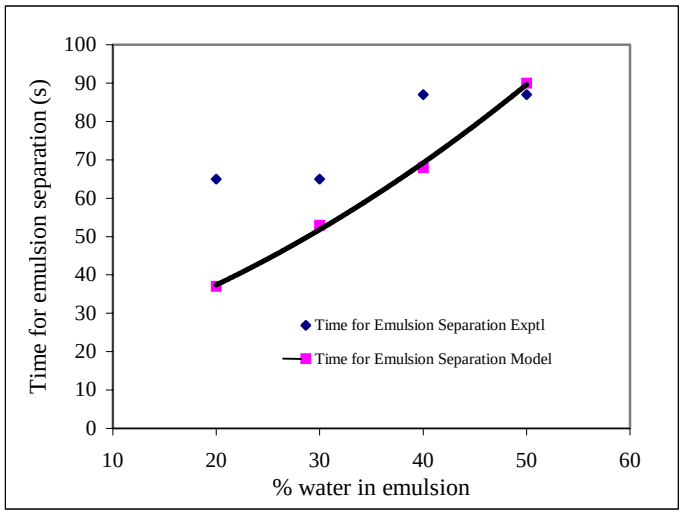


Figure 16. Comparison of model prediction of time for emulsion separation with the experimentally observed values of time for emulsion separation as a function of water content of the emulsion at a constant heat flux of 8 $kW/m^2$.

Figure 17 shows the temperature variation inside the pool as a function of distance from the pool surface at various time intervals from start of heating. Continuous lines represent the profiles obtained from the model where as the temperature values measured during the experiments are indicated by symbols. The data presented are for 50 % water in diesel emulsion heated using heat flux of 3.6 $kW/m^2$.

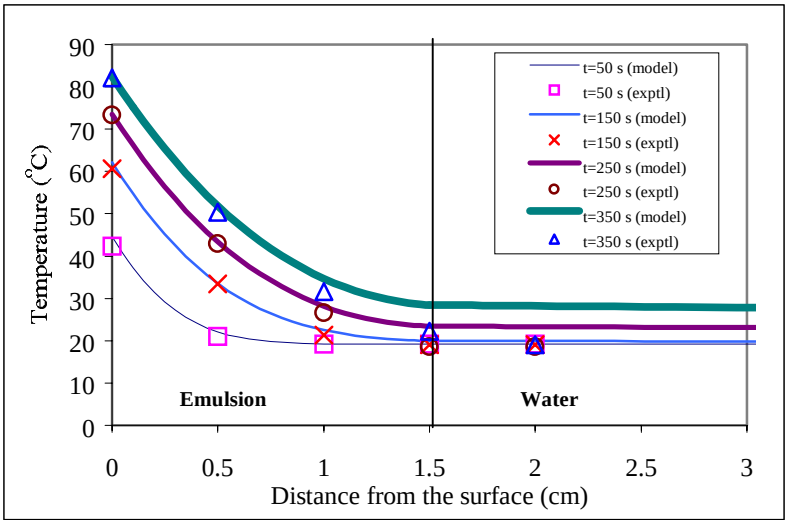


Figure 17. Comparison of model predictions of temperature profiles with the experimentally recorded values of temperatures as a function of distance from the pool surface at various time intervals from start of heating.

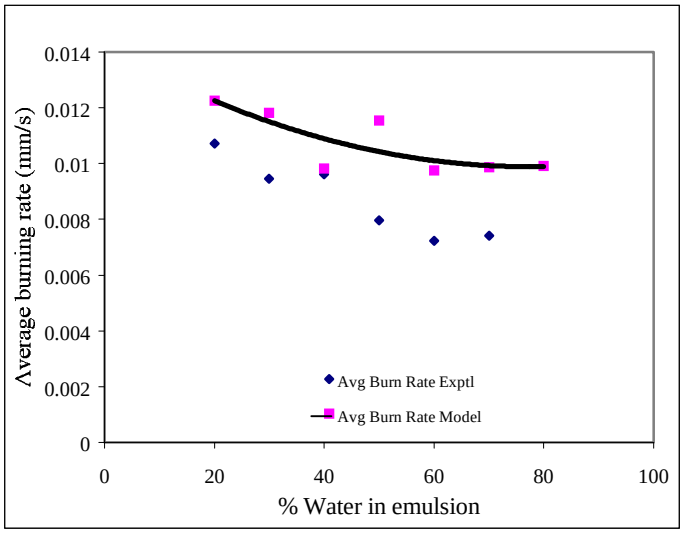


Figure 18. Comparison of average diesel burning rate predicted by the model with the experimental average diesel burning rate values as a function of water content of the emulsion at critical heat flux.

Figure 18 shows the comparison of average diesel burning rate predicted by the model with the experimental average diesel burning rate values as a function of water content of the emulsion. The average burning rate of diesel decreases with increasing water content of the emulsion. This is due to the fact that with more water in the

emulsion, there is less amount of diesel separated from the same amount of emulsion. Thus the diesel available for burning is provided at a slower rate from the emulsion layer. Hence the diesel burning rate is lower. This effect counter balances the fact that with increasing water fraction of the emulsion, the critical heat flux value will also increase, thus increasing the diesel burning rate.

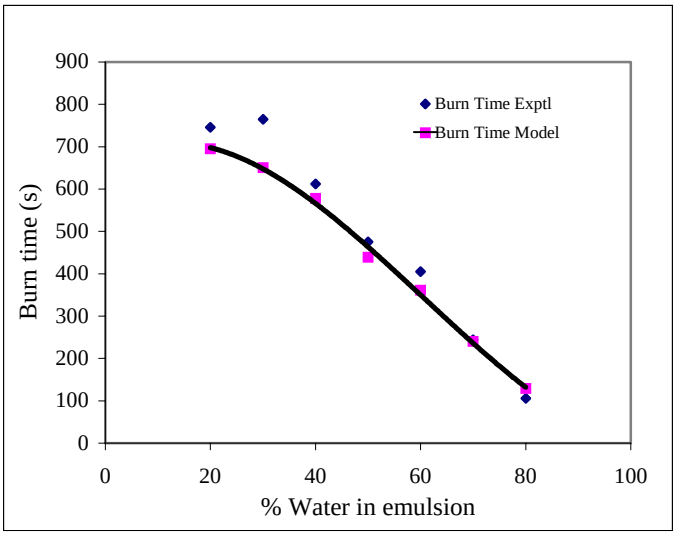


Figure 19. Comparison of the burn time predicted by the model with the experimentally observed values of burn time as a function of water content of the emulsion at critical heat flux.

Figure 19 shows the comparison of the burn time predicted by the model with the experimentally observed values of burn time for different water content of the emulsion. The burn time decreases with increasing water content of the emulsion. As the water content of the emulsion increases, for the same starting emulsion thickness, there is less amount of diesel to be burned. The latter compensates for the reduction in the average burning rate and reduces the burn time with increasing water fraction in the emulsion.

Figure 20 shows the comparison of residue thickness predicted by the model with the experimentally measured diesel residue thickness values as a function of water fraction of the emulsion. The residue thickness decreases with increasing water fraction in the emulsion. With more water in the emulsion, there is less amount of diesel to start with. Hence the diesel residue decreases with increasing water fraction of the emulsion.

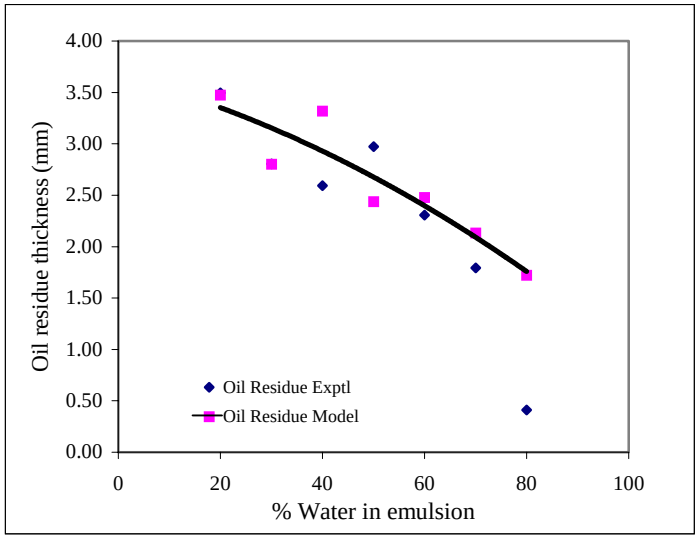


Figure 20. Comparison of diesel residue thickness predicted by the model with the experimentally measured diesel residue thickness as a function of water content of the emulsion at critical heat flux.

The comparisons of the model predictions with the experimental data indicate that the model predictions match reasonably well with the observed values. It should be noted, however, that there is a lack of accurate property data.

**Nomenclature**

| | |
|---|---|
| $C$ | Stretching factor |
| $C_o$ | Fraction of incident heat flux not absorbed at the surface |
| $C_1$ | Inverse of oil content of emulsion, on mass basis |
| $c_{po}$ | Specific heat of oil |
| $f_w$ | Fraction of water in emulsion |
| $H$ | Emulsion thickness |
| $h$ | Convective heat transfer coefficient |
| $\Delta h_{v,o}$ | Heat of vaporization for oil |
| $\Delta h_{v,w}$ | Heat of vaporization for water |
| $k$ | Thermal conductivity |
| $L$ | Oil thickness |
| $L_p$ | Rate of oil layer production due to emulsion breaking |
| $L_d$ | Rate of oil layer depletion due to oil evaporation |
| $\dot{q}''$ | Incident heat flux |
| $q_{max}$ | Maximum heat flux incident on the slick |
| $q''_r$ | Incident radiative heat flux |
| $Q_{comb}$ | Energy released by combustion of oil |

$Q_{Lo}$ Energy consumed in oil vaporization
$Q_{Lw}$ Energy consumed in water vaporization
t Time
$T_{eb}$ Emulsion breaking temperature
T Temperature
$\Delta T$ Average temperature drop across the emulsion slick
$U_O$ Overall heat transfer coefficient
$x_e$ Emulsion coordinates
$x_o$ Oil coordinates
$x_w$ Water coordinates
$y_w$ Transformed water coordinates

Greek Symbols
$\alpha$ Thermal diffusivity
$\beta$ Inverse optical depth
$\varepsilon$ Emissivity
$\rho$ Density
$\sigma$ Stefan-Boltzmann constant

Subscripts
e Emulsion
o Oil
ov Oil vaporization
w Water
1 Pertaining to initial regime
2 Pertaining to intermediate regime
3 Pertaining to final regime
i Initial conditions

## Acknowledgements

Authors would like to thank Doug Walton of National Institute of Standards and Technology, US DOC, and Joe Mullin of Mineral Management Service, US DOI, for the technical and financial support under grant no. 60NANBD0036.

## References


Arai, M., K. Saito, and R. A. Altenkirch, "Experimental Study Of Burning Liquid Fuels On A Water Sub-layer", *Symposium (International) On Combustion*, 22nd, Seattle, WA, pp.1-14, (1988).

Arai, M., K. Saito, and R. A. Altenkirch, "A Study of Boilover in Liquid Pool Fires Supported on Water Part I: Effect of Water Pool Fires", *Combustion Science and Technology*, vol. 71, pp.25-40, (1990).

Bech, C., P. Sveum, and I. A. Buist, "In-Situ Burning of Emulsions: the Effects of Varying Water Content and Degree of Evaporation", *Proceedings of the Fifteenth Arctic and Marine Oilspill Program (AMOP) Technical Seminar*, Environment Canada, Ottawa, Ontario, pp. 547-559, 1992.

Brehob, E. and Kulkarni, A. K., "Experimental Measurements of Upward Flame Spread on a Vertical Wall with External Radiation", *Journal of Fire Safety Science*,.vol. 31, pp 181-200, 1998.

Brzustowski, T. A. and E. M. Twardus, "Study of the Burning of a Slick of Crude Oil on Water", *Symposium (International) on Combustion*, 19th, (1982).

Buist, I. A., N. Glover, B. McKenzie, and R. Ranger, "In-situ Burning of Alaska North Slope Emulsions", *Proceedings of the 1995 International Oil Spill Conference*, pp.139-146, (1995).

Buist, I., and McCourt, J., 1998, "The Efficacy of In-situ Burning for Alaskan Risk Oils", Final Report, S. L. Ross Environmental Research, Ltd., (June 1998).

Evans, D. D. and E. J. Tennyson, "In-Situ Burning: A Promising Oil Spill Response Strategy", *Coastal and Ocean Management, 7th Symposium*, (1991).

Fingas, M. and N. Laroche, "Introduction to In-Situ Burning of Oil Spills", Spill Technology Newsletter, (1990).

Garo, J. P., J. P. Vantelon and A. C. Fernandez-Pello, "Experimental Study of the Burning of a Liquid Fuel Spilled on Water", *Symposium (International) on Combustion*, 25th, pp.1481-1488, (1994).

Guenette, C., P. Sveum, I. Buist, T. Aunaas, and L. Godal, "In-Situ Burning of Water-In-Oil Emulsions", SINTEF Report STF21 A94053, Reprinted as MSRC Technical Report Series 94-001, pp. 139, (1994).

Guenette, C. C., P. Sveum, C. Bech and I. Buist, "Studies of In-situ Burning of Emulsions in Norway", *Oil Spill Conference*, pp.115-122, (1995).

Hamins, A., M. E. Klassen, J. P. Gore, S. J. Fischer, and T. Kashiwagi, "Heat Feedback to the Fuel Surface in Pool Fires", *Combustion Science and Technology*, vol. 97, pp. 37-62, (1994).

Hokstad, J. N., P. S. Daling, A. Lewis, and T. Strϕm-Kristiansen, "Methodology for Testing Water-in-Oil Emulsions and Demulsifiers. Description of Laboratory Procedures", in *Formation and Breaking of Water-in-Oil Emulsions: Workshop Proceedings*, Technical Report Series, 93-018, 223-253, 1995.

Pisarchik, M., Kocis, D., Walavalkar, A. and Kulkarni, A. K., " Effect of Temperature on Breaking of Water-in-Oil Emulsions", *Twentieth Arctic and Marine Oil Spill Program Technical Seminar*, (1997), Vancouver, Canada. Also, "A Study on Water-in-Oil Emulsions and the Temperature at which They Separate", Final Report, 1997, National Science Foundation Summer Intern Program at The Pennsylvania State University, (1997).

Putorti, A. D., Jr. and D. Evans, "Ignition of Weathered and Emulsified Oils", *Proceedings of the Seventeenth Arctic and Marine Oil Spill Program Technical Seminar*, vol.1, pp. 657-667, (1994).

Strom-Kristiansen, T., A. Lewis, P. S. Daling, and A. B. Nordvik, "Demulsification by Use of Heat and Emulsion Breaker", *Proceedings of Eighteenth Arctic and marine Oil Spill Program Technical Seminar*, vol. 1, pp. 367-384, (1995).

Tien, C. L., "Radiative Modeling of Pool Fires," *Summaries of center for Fire Reseach Grants and In-House Programs – 1986*, National Institute of Standards and Technology, Gaithersburg, MD.

Thompson, C. H., G. W. Dawson, and G. L. Goodier, "Combustion: An Oil Spill Mitigation Tool", US Department of Energy, Washington, DC, pp. 53, (1979).

Vargaftik, N. B., "Tables on the Thermophysical Properties of Liquids and Gases", 2nd Edition, Hemisphere Publication Corporation, pp. 695, (1975).

Walavalkar, A. and A. K. Kulkarni, "A Comprehensive Review of Oil Spill Combustion Studies", *Proceedings of the Nineteenth Arctic and Marine Oil Spill Program Technical Seminar*, pp. 1081-1103, (1996).

Walavalkar, A. and A. K. Kulkarni, "A Mathematical Model for In-Situ Burning of Water-in-Oil Emulsions", *Proceedings of the Twentieth Arctic and Marine Oil Spill Program Technical Seminar*, pp 809-821, (1997).

Wu, N., M. Baker, G. Kolb, and J. L. Torero, "Ignition, Flame Spread and Mass Burning Characteristics of Liquid Fuels on a Water Bed", *Proceedings of Twentieth Arctic and Marine Oil spill Program Technical Seminar*, vol. 2, pp. 769-793, (1997).

Yamaguchi, T. and Wasaka, K., "Oil Pool Fire Experiment," *Fire Safety Science - Proceedings of the First International Symposium*, p 911, 1986.